

Activity waves in binary active colloids of Quincke rollers

Yuan Xie(谢圆), Xiao-Yi Zhou(周晓怡), Qi-Ying Ni(倪琦英), Wen-De Tian(田文得), Kang Chen(陈康), and Tian-Hui Zhang(张天辉)

Citation: Chin. Phys. B, 2025, 34 (**12**): 126401. DOI: 10.1088/1674-1056/ae07ae
http://cpb.iphy.ac.cn; http://iopscience.iop.org/cpb

What follows is a list of articles you may be interested in

Aligning and flocking of ellipsoidal Quincke rollers by flipping

Kai-Xuan He(何凯旋), Qi-Ying Ni(倪琦英), Xiao-Yi Zhou(周晓怡), Wen-De Tian(田文得), Kang Chen(陈康), and Tian-Hui Zhang(张天辉)

Chin. Phys. B, 2025, 34 (**7**): 076401. DOI: 10.1088/1674-1056/adc669

Learning physical states of bulk crystalline materials from atomic trajectories in molecular dynamics simulation

Tian-Shou Liang(梁添寿), Peng-Peng Shi(时朋朋), San-Qing Su(苏三庆), and Zhi Zeng(曾志)

Chin. Phys. B, 2022, 31 (**12**): 126402. DOI: 10.1088/1674-1056/ac98a4

Solid-to-molecular-orientational-hexatic melting induced by local environment determined defect proliferations

Zhanglin Hou(侯章林), Jieli Wang(王杰利), Ying Zeng(曾颖), Zhiyuan Zhao(赵志远), Xing Huang(黄兴), Kun Zhao(赵坤), and Fangfu Ye(叶方富)

Chin. Phys. B, 2022, 31 (**12**): 126401. DOI: 10.1088/1674-1056/ac8ce1

Anomalous bond-length behaviors of solid halogens under pressure

Min Wu(吴旻), Ye-Feng Wu(吴烨峰), and Yi Ma(马毅)

Chin. Phys. B, 2021, 30 (**7**): 076401. DOI: 10.1088/1674-1056/abf4bd

Novel structures and mechanical properties of Zr_2N: *Ab initio* description under high pressures

Minru Wen(文敏儒), Xing Xie(谢兴), Zhixun Xie(谢植勋), Huafeng Dong(董华锋), Xin Zhang(张欣), Fugen Wu(吴福根), and Chong-Yu Wang(王崇愚)

Chin. Phys. B, 2021, 30 (**1**): 016403. DOI: 10.1088/1674-1056/abb220

Activity waves in binary active colloids of Quincke rollers

Yuan Xie(谢圆)[†], Xiao-Yi Zhou(周晓怡)[†], Qi-Ying Ni(倪琦英)[†],
Wen-De Tian(田文得)[‡], Kang Chen(陈康)[§], and Tian-Hui Zhang(张天辉)[¶]

Center for Soft Condensed Matter Physics and Interdisciplinary Research & School of Physical Science and Technology, Soochow University, Suzhou 215006, *China*

(Received 27 April 2025; revised manuscript received 10 June 2025; accepted manuscript online 17 September 2025)

Activity waves are popular in excitable systems. Here, we show that binary active colloids of Quincke rollers driven by an alternating electric field can also form activity waves. In the activity waves, Quincke rollers exhibit a memory of the direction of motion. This memory occurs at frequencies much smaller than that in monodisperse systems. It is found that the enhanced memory arises from the paired distinct rollers which break the dynamic symmetry because of the configuration-dependent dipole–dipole interactions. This finding demonstrates that dipole–dipole interactions between distinct active agents can significantly modify the collective dynamics of polydisperse active systems.

Keywords: polydisperse active systems, activity waves, dipole–dipole interactions

PACS: 64.60.–i, 05.65.+b, 87.18.Gh, 82.70.Dd

DOI: 10.1088/1674-1056/ae07ae **CSTR:** 32038.14.CPB.ae07ae

1. Introduction

Activity waves are ubiquitous in excitable media,[1–3] including chemical,[4] physical,[5] and biological systems.[6] In biological systems, local stimulation excite signal waves-which play a crucial role in information transmission.[7–9] For example, action potential waves[10–13] propagate directionally through nerve fibers, enabling intercellular signal transmission. During embryonic development, morphogens form continuous concentration gradient waves,[14–17] determining different cell differentiation directions. Calcium ion oscillation waves[18–21] specifically regulate numerous vital physiological processes such as gene expression and cell division through spatiotemporal encoding. Understanding the excitation and regulation mechanisms of activity waves is not only essential for revealing the dynamic laws of life systems but also provides a theoretical framework for designing bionic intelligent materials. To uncover the microscopic dynamics underlying activity waves, active colloids have been employed as an experimental model in the study of activity waves.[22,23] For instance, silver colloid particles form directed ballistic waves via photophoretic swimming triggered by hydrogen peroxide decomposition in a light field; under high-density conditions, they form swarming waves through diffusiophoretic flows.[24] In Quincke systems, sub-critical waves can be excited due to Quincke instability.[25] As Quincke rollers are driven by an alternating fields, density-dependent memory can also induced activity waves.[26] These observations show that active colloids can also serve as excitable systems.

In nature, active agents are generally polydisperse in physical properties. Distinct agents often exhibit different individual particle dynamics, such as self-propulsion speeds,[27–29] diffusion coefficients,[30] and polydisperse interactions.[31] Nevertheless, the effect of polydispersity on collective behaviors and the exciting of activity waves have so far not been addressed. Here, in this study, a binary active system of Quincke rollers with two particle sizes driven by an alternating electric field are employed to explore the effect of polydispersity on collective dynamics. It is found that because of the stronger dipole–dipole attraction between the large particle and the small particle, the memory of the direction of propulsion occurs at frequencies much lower than that observed in monodisperse Quincke systems, and results in activity waves in active liquid.

2. Experimental methods

In our experiments, a binary colloidal system is prepared with polystyrene particles of two diameters 10 μm and 6 μm are mixed with a number ratio 1:1 and dispersed in a 0.15-mol/L mixture of sodium di-2-ethylhexylsulfosuccinate (AOT) and hexadecane (Fig. 1(a)). The solution is then sealed in a cell constructed of two indium tin oxide (ITO)-coated glass slides separated by a square boundary. Due to the higher density of the particles compared to the solvent, they settle on the bottom electrode, forming a quasi-two-dimensional monolayer.

A periodic square-wave electric field (SWE) is applied

[†]These authors contributed equally to this work.
[‡]Corresponding author. E-mail: tianwende@suda.edu.cn
[§]Corresponding author. E-mail: kangchen@suda.edu.cn
[¶]Corresponding author. E-mail: zhangtianhui@suda.edu.cn

© 2025 Chinese Physical Society and IOP Publishing Ltd. All rights, including for text and data mining, AI training, and similar technologies, are reserved.

perpendicular to the electrode surface. The magnitude E alternates between a peak value E_p ($> E_c$) and a valley value E_g ($= 0$). The durations for off-period (E_g) and on-period (E_p) are equal in one cycle. When the electric field exceeds the critical threshold E_c, the particles undergo Quincke rotation: the dipole moment P is disturbed from its equilibrium state by fluctuations, an in-plane component $P_\perp$ arises, leading to a destabilizing torque $P_\perp \times E$, which overcomes the viscous resistance of liquid and induces rotational motion.[32] Notably, the critical field E_c for 6-μm particles is lower than that for 10-μm particles due to their smaller size ($E_C = [4\pi\varepsilon_l a^3(\chi^\infty + \frac{1}{2})\mu_r\tau]^{-1/2}$, where a is the particle radius[32]); all E_c values reported here correspond to the 10-μm particles. In the steady state, the translational speed is dependent on by $E_C v \sim \sqrt{(E/E_C)^2 - 1}$.[33]

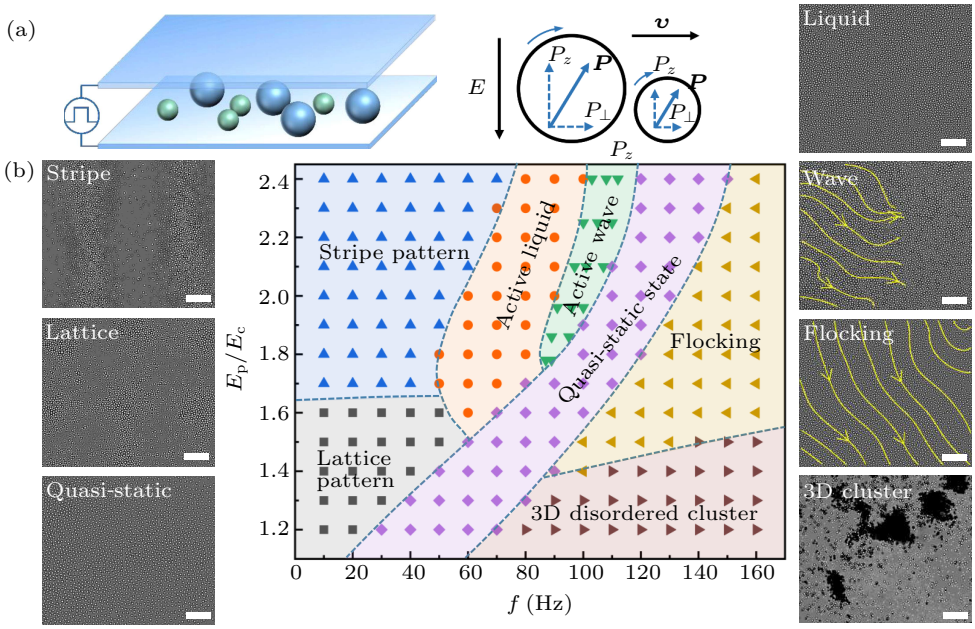


Fig. 1. (a) Schematic diagram of the experimental setup; (b) Phases in the system: oscillating lattice pattern ($E_p = 1.39E_c$, $f = 10$ Hz); oscillating stripe pattern ($E_p = 1.78E_c$, $f = 10$ Hz); quasi-static phase ($E_p = 2.02E_c$, $f = 113$ Hz); active liquid ($E_p = 1.94E_c$, $f = 85$ Hz); activity wave ($E_p = 1.96E_c$, $f = 99$ Hz); flocking ($E_p = 1.85E_c$, $f = 160$ Hz); three-dimensional (3D) disordered clusters ($E_p = 1.3E_c$, $f = 9$ Hz). The yellow lines in the figure represent streamlines. The scale bar is 100 μm.

3. Results

The binary system exhibits a rich variety of phases by adjusting the peak E_p and frequency f as shown in Fig. 1(b). At low frequencies (< 20 Hz), dynamic patterns including square lattices and stripes form (see Movies 1(a) and 1(b)) as reported in our previous studies.[34] Unlike monodisperse systems, these patterns are not regular as that observed in monodisperse systems due to the different mobility of large and small particles. Large particles move faster than small ones, so their travel distance is larger in one cycle. As the frequency increases, the travel distance of particles in each cycle decreases such that macroscopic patterns disappear. The mechanism is that long-distance diffusion and macroscopic density fluctuation are necessary to form macroscopic patterns. As the travel distance in each cycle is smaller than the mean distance between particles, macroscopic density fluctuations are suppressed and a quasi-static state emerges (see Movie 1(c)).

As the frequency is high enough such that the off-period of E is less than the charge relaxation time, Quincke rollers exhibit a memory of the direction of propulsion and their motion becomes persistent in direction, although they are propelled intermittently. As a result, flocking emerges (see Movie 1(d)). Moreover, it is noticed that upon the increase of frequency, the mobility of Quincke rollers decreases because of the reduced acceleration time in one cycle.[26] In this case, Quincke rollers can form condensed active phases due to the longrange attraction induced by electrohydrodynamic (EHD) flows. At higher frequencies, as the mobility is further reduced, the quasi-static Quincke rollers form static 3D disordered clusters at small E_p due to the dipole–dipole interactions along the direction of E (see Movie 1(e)).

Between the stripe phase and the quasi-static phase, there is a transition region where patterns do not disappear entirely: dynamical dense clusters form and oscillate with E (see Movie 1(f)). The formation of dense clusters leads to local density fluctuations. The density in active liquid is not uniform (Fig. 2(a)). Trajectories show that Quincke rollers in the active liquid exhibit Brownian motion (Fig. 2(b)). Mean squared displacements (MSD) reveal that at short time scale ($< T$), the motion is ballistic ($\langle \Delta r^2 \rangle \propto t^2$) (Fig. 2(c)) while at long time scales ($> T$), it is typical Brownian motion ($\langle \Delta r^2 \rangle \propto t$). It follows that Quincke rollers in the dynamical cluster phase

behave like liquid particles. In this sense, the dynamic cluster phase exhibits liquid characteristics, namely, active liquid. Nevertheless, distinct from conventional liquid, a well-directed wave can be excited and propagate in the active liquid (Movie 1(g)). The activity waves originate from local density fluctuations, which create local denser regions (Figs. 3(a)–3(b) and Movie 2). The velocity of the wave particles is much higher than that in the liquid background (Figs. 3(c) and 3(d)).

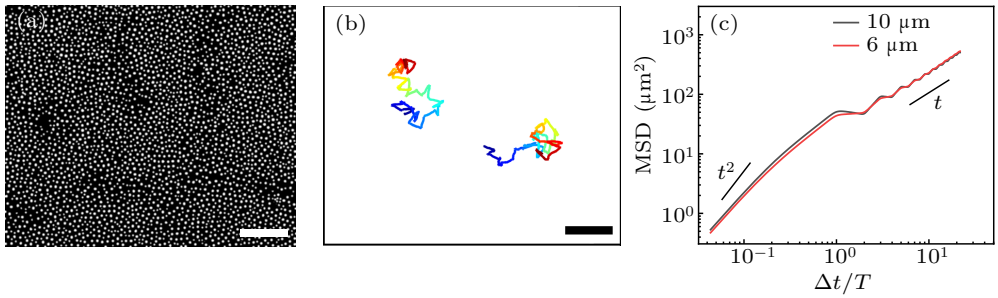


Fig. 2. Active liquid under periodic electric field ($E_p = 1.9E_c$, $f = 85$ Hz). (a) Snapshot of active liquid. (b) Typical trajectories of active liquid particles within one second: a small particle (left) and a large particle (right). (c) Means squared displacements (MSD). The scale bar in panel (a) is 100 μm. The scale bar in panel (b) is 28 μm.

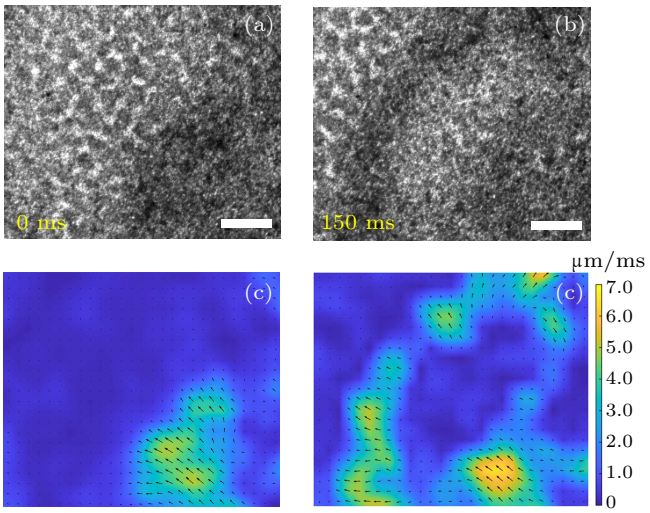


Fig. 3. Emergence of activity waves under periodic square-wave electric field ($E_p = 2.15E_c$, $f = 101$ Hz). (a)–(b) Snapshots of the emergence of waves. (a) At 0 ms, local fluctuations in the lower-right corner excite waves. (b) After 150 ms, the activity wave propagates through the active liquid towards the upper-left direction in the figure. (c)–(d) The corresponding velocity fields of panels (a) and (b). The scale bar is 500 μm.

The density at the wave front decreases, resulting in a boundary between the wave and the liquid. When the electric field E is switched off, the wave structure is retained (Figs. 4(a) and 4(d) up), and the velocities of particles in both the active liquid and the activity wave drop to zero (Fig. 4(d) bottom). Upon the electric field E switched on again, particles are reactivated, and those within the wave are propelled forward in a common direction (Figs. 4(b) and 4(c)). The density of particles in the wave, ϕ is around 0.7, which is higher than the local area fraction in active liquids (Figs. 4(e) and 4(f)). By tracking the wave front positions in different cycles, the average wave speed is measured to be around 6.32 μm/ms, which exceeds the maximum instantaneous velocity of particles in the liquid and is close to the maximum instantaneous velocity of particles within the wave (Fig. S1 up). However, the motion of particles within the wave bands exhibits intermittent characteristics, enabling waves to propagate a longer distance per cycle than individual particle displacements. When particles become incorporated into the wave front, the local area fraction increases significantly (Fig. S1 bottom). Particles remain trapped within the wave structure for multiple cycles before detaching. After the wave passes, the local active liquid spontaneously recovers.

Particles in the active liquid exhibit Brownian motion, indicating no persistence in their direction of motion. In the wave, particle velocities periodically drop to zero as well. Despite this, however, particles in the wave maintain their direction of motion. It follows that wave particles have a memory of the direction of motion. This memory is absent in the low-density active liquid. Previous studies have shown that when the electric field is switched off for a time shorter than the charge relaxation time, Quincke rollers retain a memory of their propulsion direction.[35] This memory can be enhanced in dense clusters due to the dipolar interactions between the Quincke rollers.[26]

To confirm the role of memory in the propagation of activity waves, we froze the wave by turning off the electric field for a long time (> 30 minutes), to assure that the dipole moment in the particle is relaxed completely. Upon reapplying the electric field, particles in the frozen wave diffuse into the surrounding active liquid in both directions (forward and backward) due to dipole–dipole repulsion. The dense band of wave disappears gradually (Fig. 5 and Movie 3). This confirms that complete charge relaxation is responsible for the directed motion of wave.

For individual Quincke rollers, the charge relaxation time is determined by $\tau_{MW} = (\varepsilon_p + 2\varepsilon_l)/(\sigma_p + \sigma_l)$ (the permittivities ε and conductivities σ of particle (p) and liquid (l)), and is estimated as 4 ms.[36] Therefore, the memory occurs only when the frequency is above 250 Hz where the electric field

switching period becomes shorter than the polarization relaxation time.[26] In a dense cluster, however, because of the enhanced dipole–dipole interactions between closely packed particles, the charge relaxation process is significantly delayed due to the persistent local electric fields generated by neighboring dipoles. Consequently, the memory in dense clusters occurs at lower frequencies ($\sim$ 185 Hz). Nevertheless, in this study, the activity waves occur at much lower frequencies ($f < 100$ Hz). It follows that the charge relaxation in binary systems is even slower than that in monodisperse systems.

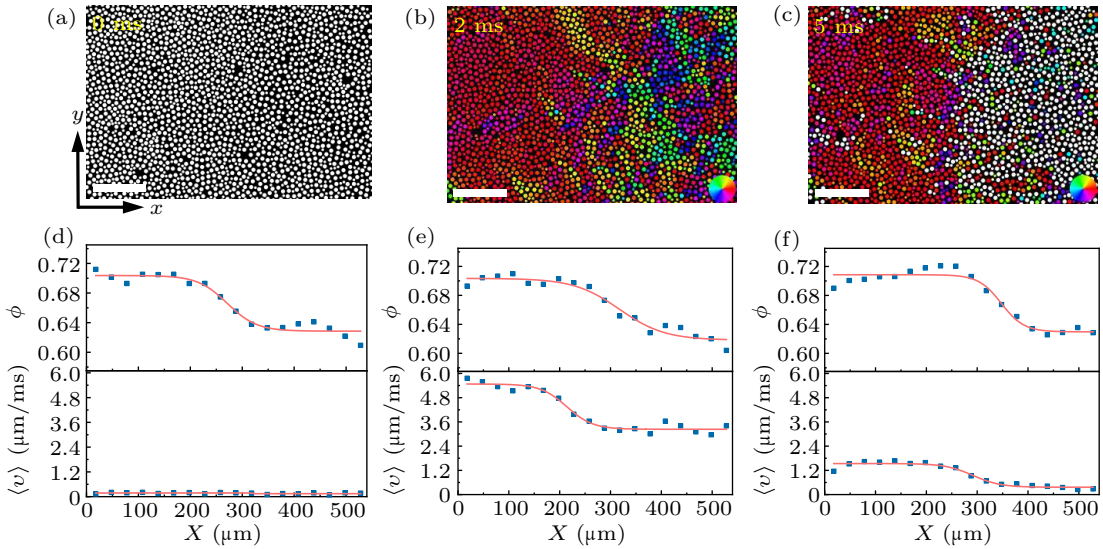


Fig. 4. Evolution of velocity and density within one period of a wave in the active liquid ($E_p = 1.96E_c$, $f = 99$ Hz). (a)–(c) Snapshots with particles colored by the direction of velocity. (a) At the static state (0 ms). (b) 2 ms after activation of E_p. (c) At the end of E_p (5 ms). X-axis denotes wave propagation direction. (d)–(f) Local particle density (ϕ) and velocity ($\langle v \rangle$) distribution of 6-μm and 10-μm particles in the wave, which are averaged over Y. The red lines are the fitting curves of the data points. The scale bar in panels (a)–(c) is 100 μm.

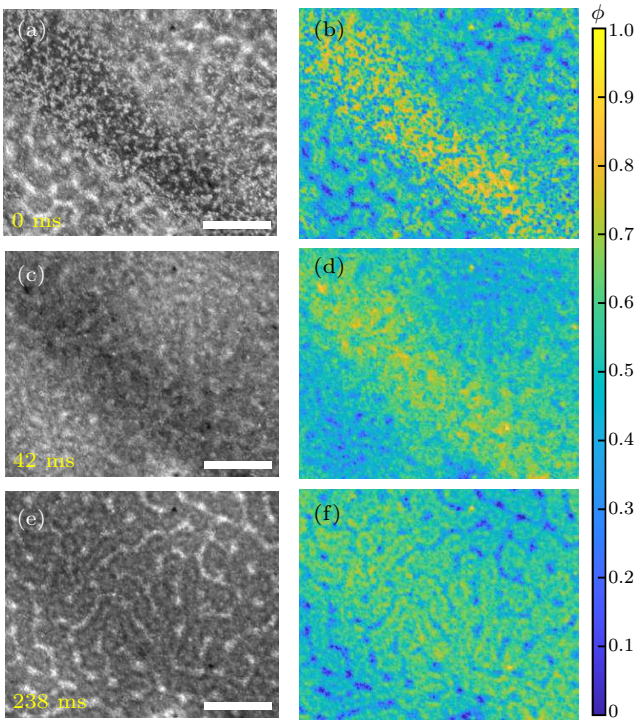


Fig. 5. Dissociation of activity wave after freezing ($E_p/E_c = 2.3$, $f = 103$ Hz). (a), (c), and (e) Snapshots of the wave. (b), (d), and (f) The corresponding density-colored snapshots of panels (a), (c), and (e). (a) All particles are stationary, and the wave is frozen (0 ms). (c) 42 ms after the electric field is applied, the activity wave ceases to propagate, indicating memory loss. (e) 238 ms after the electric field is applied, the wave structure dissipates entirely into the active liquid. The scale bar is 500 μm.

The delayed relaxation of charge arises from the attractive interactions between the in-plane dipoles (Fig. 1(a)). Nevertheless, the interaction between $P_\perp$ is short-ranged compared with the repulsive interactions between P_z. Therefore, it occurs only in a dense structure. The attractive dipolar interaction can enhance the rotation torque and activate Quincke rotation at subcritical E,[25] and delay the charge relaxation in dense clusters of Quincke rollers.[26,37] For two Quincke rollers of different sizes but located on the same plane, the dipolar repulsion will be reduced (Fig. 6(a)). To quantify the dipolar interactions between two Quincke rollers, the interaction potential energy is calculated with a simplified dipole model (Fig. S2). The results show that compared with the interaction between two identical large Quincke rollers, the interaction energy between a large roller and a small roller is much lower. More importantly, it is found that as the large roller is located ahead of the small one, the interaction energy is much lower than that as the small one is ahead the large one. Nevertheless, in our calculations, the charge of small particles is 2.778 times less than the large particle. Therefore, the reduced potential energy may be induced by the less charge of small particle. To exclude the effect of charge quantity, the potential energy is calculated with the assumption that small particles have the same charge as that of large particles. The results (blue lines in Fig. 6(a)) show that the potential energy is still universally less than that between two identical large particles as the large particle is followed by a small particle with the same charge. It follows that as the small particles roll behind the large one, the attractive interaction between the in-plane dipole components

is stronger than that between two identical large particles. A stronger attraction between charges leads to slower relaxation of dipoles. This explains why the frequency for memory in the binary system is much smaller than that in monodisperse system.

The remaining dipole moments in the wave not only maintain a memory of the direction of propulsion but also result in a faster acceleration of Quincke rollers in each cycle. It is found that as E_p is restarted, the speed of rollers in wave increases faster and reaches a peak value higher than that in liquid (Fig. 6(b)). Because of the viscosity of the solvent, the compressed structures of AOT produce an elastic force which impedes the motion of Quincke rollers,[26] giving rise to the sharp decrease of speed. As the deformation of solvent is relaxed, the rollers will be reactivated. The speed of rollers in wave exhibits an obvious reacceleration before the electric field drops to zero. By contrast, the rollers in liquid do not experience a reacceleration after the first peak value. These observations suggest that the rotation torque in wave is much stronger than that in liquid. This offers additional evidence that the in-plane dipole component in wave is stronger than that in active liquid.

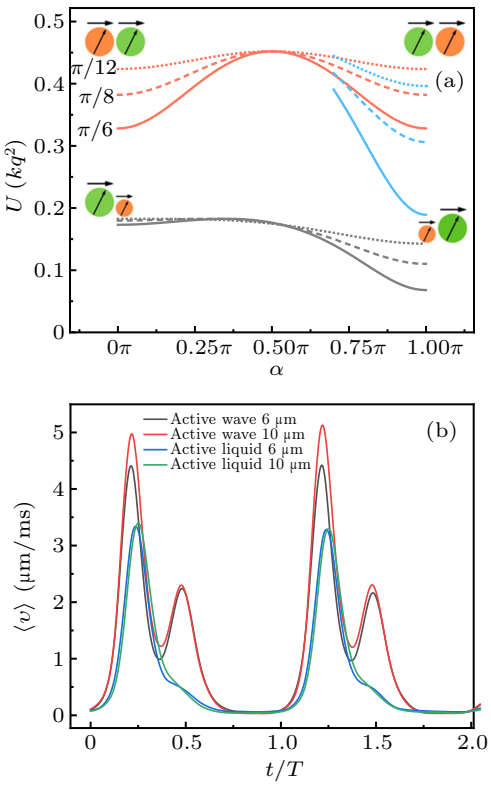


Fig. 6. (a) Potential energy-conformation diagram for particles of different sizes with different dipole tilt angles. Red lines: the potential energy of two large particles. Grey lines: the potential energy of a large particle and a small particle. Blue lines: the potential energy of a large particle and a small particle (assuming the charge of the small particle is the same as that of the large particle). (b) Average velocity-time relationship for particles in and outside waves.

In summary, the dipole–dipole interactions between distinct Quincke rollers induces a memory which occurs at frequencies lower than that observed in monodisperse systems. This enhanced memory arises from the enhanced attractive interaction between in-plane dipole components. This finding suggests that in polydisperse active systems, dipole–dipole interactions between distinct active agents can significantly modify the collective dynamics and enrich the results of self-organization in non-equilibrium systems.

Acknowledgement

Project supported by the National Natural Science Foundation of China (Grant No. 11974255).

References

[1] Keener J P 1980 *SIAM J. Appl. Math.* **39** 528
[2] Meron E 1992 *Phys. Rep.* **218** 1
[3] Zykov V S 2018 *Philos. T. R. Soc. A* **376** 20170379
[4] Cassani A, Monteverde A and Piumetti M 2021 *J. Math. Chem.* **59** 792
[5] Malomed B A and Mihalache D 2019 *Rom. J. Phys.* **64** 106
[6] Deneke V E and Di Talia S 2018 *J. Cell Biol.* **217** 1193
[7] Inagaki N and Katsuno H 2017 *Trends Cell Biol.* **27** 515
[8] Driscoll M K, McCann C, Kopace R, *et al.* 2012 *PLoS Comput. Biol.* **8** e1002392
[9] Allard J and Mogilner A 2013 *Curr. Opin. Cell Biol.* **25** 107
[10] Drukarch B Wilhelmus M M and Shrivastava S 2022 *Rev. Neurosci.* **33** 285
[11] Bouchard R A, Clark R B and Giles W R 1995 *Circ. Res.* **76** 790
[12] Beeler G W and Reuter H 1977 *J. Physiol.* **268** 177
[13] Bean B P 2007 *Nat. Rev. Neurosci.* **8** 451
[14] Wartlick O, Jülicher F and Gonzalez-Gaitan M 2014 *Development* **141** 1884
[15] Harrison L G, Snell J, Verdi R, *et al.* 1981 *Protoplasma* **106** 211
[16] Christian J L 2012 *WIREs Dev. Biol.* **1** 3
[17] Bressloff P C 2022 *Phys. Biol.* **19** 066005
[18] Sneyd J, Keizer J and Sanderson M J 1995 *FASEB J.* **9** 1463
[19] Ross W N 2012 *Nat. Rev. Neurosc.* **13** 157
[20] Parkash J and Asotra K 2010 *Life Sci.* **87** 587
[21] Jaffe L 1993 *Cell Calcium* **14** 736
[22] Zhang T H, Groenewold J and Kegel W K 2009 *Phys. Chem. Chem. Phys.* **11** 10827
[23] Zhang T H and Liu X Y 2014 *Chem. Soc. Rev.* **43** 2324
[24] Chen X, Xu Y, Zhou C, *et al.* 2022 *Sci. Adv.* **8** eabn9130
[25] Liu Z T, Shi Y, Zhao Y, *et al.* 2021 *Proc. Natl. Acad. Sci. USA* **118** e2104724118
[26] Yang Y, Zhang M F, Zhu L, *et al.* 2023 *Chin. Phys. Lett.* **40** 126401
[27] Adhikary S and Santra S 2022 *Phys. Rev. E* **105** 064612
[28] Kolb T and Klotsa D 2020 *Soft Matter* **16** 1967
[29] Pattanayak S, Singh J P, Kumar M, *et al.* 2020 *Phys. Rev. E* **101** 052602
[30] Kumari S, Nunes A S, Araújo N A, *et al.* 2017 *J. Chem. Phys.* **147** 174702
[31] Maity S and Morin A 2023 *Phys. Rev. Lett.* **131** 178304
[32] Bricard A, Caussin J B, Desreumaux N, *et al.* 2013 *Nature* **503** 95
[33] Das D and Saintillan D 2013 *Phys. Rev. E* **87** 043014
[34] Yang Y, Zhang Z C, Qi F, *et al.* 2022 arXiv: 2204.07717
[35] Karani H, Pradillo G E and Vlahovska P M 2019 *Phys. Rev. Lett.* **123** 208002
[36] Jones T B A 1984 *IEEE Trans. Ind. Appl.* **IA-20** 845
[37] Zhang M F, Fan B Y, Zhang C Y, *et al.* 2025 *Soft Matter* **21** 927